Effects of entrainment on convective available potential energy and closure assumptions in convection parameterization

Guang J. Zhang[1]

Received 12 August 2008; revised 19 January 2009; accepted 9 February 2009; published 10 April 2009.

[1] This study investigates the effect of entrainment dilution on convective available potential energy (CAPE) and closure assumptions in convection parameterization using the sounding data from three Intensive Observation Periods (IOPs). It is shown that entrainment of the environmental air has a strong dilution effect on CAPE, and this effect depends on the degree of subsaturation of the entrained air: the drier the entrained air, the larger the effect. For CAPE-based closure assumptions, the dilute CAPE has a moderate correlation with convective removal of CAPE. While better than for undiluted CAPE, which is virtually uncorrelated with convective CAPE removal, this correlation is not satisfactory enough for convection closure. For quasi-equilibrium–based closures, while the free tropospheric quasi-equilibrium assumption is a superior closure for convection when undiluted CAPE is used, both the Arakawa-Schubert quasi-equilibrium closure and the free tropospheric quasi-equilibrium closure work well for dilute CAPE in all three IOPs studied. It is further shown from the CAPE definition and the large-scale temperature budget equation that for undiluted CAPE, the free tropospheric large-scale CAPE change and precipitation are approximately linearly related. The most important effect of entrainment dilution on CAPE and convection parameterization closure assumptions is to enhance the role of free tropospheric humidity, thereby diminishing the overwhelming role of boundary layer control on undiluted CAPE and its variation.

Citation: Zhang, G. J. (2009), Effects of entrainment on convective available potential energy and closure assumptions in convection parameterization, *J. Geophys. Res.*, *114*, D07109, doi:10.1029/2008JD010976.

1. Introduction

[2] Convection parameterization in global climate models (GCM) is among the most challenging problems facing the climate modeling community [*Arakawa*, 2004]. The simulation of many climate systems, particularly in the tropics, such as the Madden-Julian oscillation, the Intertropical Convergence Zone, and the El Nino-Southern Oscillation, is very sensitive to how convection is represented in the models [*Maloney and Hartmann*, 2001; *Zhang and Mu*, 2005; *Zhang and Wang*, 2006; *Li and Zhang*, 2008]. Among the many assumptions in a convection parameterization, e.g., convection trigger, closure, lateral entrainment and detrainment, microphysics and rainwater conversion, etc., convection closure is probably the most fundamental and least understood theoretically and observationally. It is used to determine how much convection occurs given the large-scale atmospheric conditions. Widely used convection closures in GCMs include those based on low-level moisture convergence [*Tiedtke*, 1989], convective available potential energy (CAPE) [*Zhang and McFarlane*, 1995; *Gregory et al.*, 2000], and the quasi-equilibrium between convection and the large-scale forcing on CAPE [*Arakawa and Schubert*, 1974; *Zhang*, 2002]. Although CAPE is generally considered a qualitative measure of convective activity from the thermodynamic point of view, that is, if released it provides energy for convective overturning of the air, its calculation is subject to many arbitrary assumptions, which lead to large uncertainties in CAPE values. For instance, the level of origin of the air parcel being lifted in CAPE calculation can have significant impact on CAPE values [*Emanuel*, 1994]. Furthermore, observational studies indicate that CAPE variability is largely determined by thermodynamic properties of the boundary layer [*McBride and Frank*, 1999; *Zhang*, 2002, 2003; *Donner and Phillips*, 2003]. On the other hand, a number of studies have indicated that lower tropospheric moisture can have important effect on convection [*Raymond*, 1995; *Michaud*, 1998; *Neelin et al.*, 2008; *Holloway and Neelin*, 2009]. Drier air in the lower troposphere often makes it more difficult for deep convection to occur than a moister lower troposphere due to entrainment. To take this effect into account, recently the Atmospheric Model Working Group (AMWG) of the National Center for Atmospheric Research Community Climate System Model (NCAR CCSM3) included entrainment dilution in CAPE calculation in an experimental version of the atmospheric model CAM3.5 [*Neale et al.*, 2008]. Conceptually, the dilute CAPE is similar to the cloud work function of *Arakawa and Schubert* [1974]; it is the vertical integral of a parcel's buoyancy weighted by entrainment.

[1]Climate, Atmospheric Science and Physical Oceanography Division, Scripps Institution of Oceanography, University of California, San Diego, La Jolla, California, USA.

0148-0227/09/2008JD010976

[3] *Zhang* [2002, 2003] examines observational data from soundings in both the tropics and midlatitudes and finds that the conventional quasi-equilibrium assumption of *Arakawa and Schubert* [1974] does not adequately describe the relationship between large-scale generation and convective consumption of CAPE. On the basis of the analysis, he proposed a free tropospheric quasi-equilibrium closure assumption using large-scale CAPE forcing [*Xie and Zhang*, 2000]. *Donner and Phillips* [2003] compare observations from the GARP Atlantic Tropical Experiment (GATE), the Tropical Ocean Global Atmosphere Coupled Ocean-Atmosphere Response Experiment (TOGA COARE), and the Atmospheric Radiation Measurement (ARM) Southern Great Plains site summer 1997 Intensive Observation Period (SGP97 IOP) with three closure assumptions. They find that of the three closure assumptions (the CAPE relaxation closure, the Arakawa-Schubert quasi-equilibrium closure and the free tropospheric quasi-equilibrium closure), the free tropospheric quasi-equilibrium agrees the closest with the observations. Tests of the free tropospheric quasi-equilibrium in the Zhang-McFarlane scheme show many improvements in the simulation of the tropical climate in the NCAR CCM3, CAM3 and CCSM3 [*Zhang and Mu*, 2005; *Zhang and Wang*, 2006; *Li and Zhang*, 2008]. However, one drawback of the assumption is that it does not explicitly consider the boundary layer influence other than requiring positive CAPE to satisfy the necessary condition for convection. This may lead to underprediction and wrong timing of convection (e.g., diurnal cycle) in regions where thermal forcing in the boundary layer is an important mechanism for convection such as the southeast US and the North American Monsoon region [*Collier and Zhang*, 2006]. Consideration of entrainment dilution in CAPE calculation may be a way to remedy this defect.

[4] In this study, we examine the effect of entrainment dilution on CAPE calculation and three closure assumptions that involve CAPE calculation: the CAPE-based closure in the study by *Zhang and McFarlane* [1995], the free tropospheric quasi-equilibrium closure [*Zhang*, 2002] and the conventional quasi-equilibrium [*Arakawa and Schubert*, 1974]. Section 2 will present the data and analysis method. Section 3 presents the results. Section 4 attempts to provide a theoretical interpretation of the observed results. A summary and discussion are given in section 5.

2. Data and Analysis Method

[5] The data used for this study are the forcing data for cloud-resolving and single-column models, derived from soundings during TOGA COARE, SGP97 IOP and the Tropical Warm Pool International Cloud Experiment (TWP-ICE). The first two data sets have been used in the study by *Zhang* [2003]. The COARE data are obtained from R. H. Johnson of Colorado State University [*Ciesielski et al.*, 1997], available at 6 hourly resolution covering the period from 1 November 1992 to 28 February 1993. The SGP97 and TWP-ICE data are provided by the ARM Cloud Modeling Group through S. Xie of Lawrence Livermore National Laboratory, available at 3 hourly resolution. The SGP data covers 29 days from 19 June to 18 July 1997. Both the COARE and SGP data were discussed in more detail in the study by *Zhang* [2003]. The TWP-ICE field campaign took place in Darwin, Australia during the Australian Monsoon season for 24 days from 19 January to 12 February 2006 [*May et al.*, 2008]. During the IOP, the large-scale circulation went through wet monsoon, suppressed convection and break monsoon phases.

[6] The analysis approach follows the study by *Zhang* [2002], except that entrainment dilution is included in all calculations involving CAPE or its components and their changes with time. By definition, CAPE is the vertical integral of buoyancy of an air parcel lifted from the boundary layer to the neutral buoyancy level:

$$CAPE = \int_{p_t}^{p_b} R_d (T_{vp} - T_{ve}) d \ln p \tag{1}$$

where T_{vp} and T_{ve} are the parcel's and its environment's virtual temperature. R_d is the gas constant for air, p_b and p_t are the pressure of the parcel's originating level and neutral buoyancy level, respectively. The parcel's temperature calculation with or without entrainment in principle follows the approximation presented in the appendix of the study by *Zhang and McFarlane* [1991]. However, to avoid any numerical approximation differences from the CAM3.5 model, we use the CAM3.5 code instead [*Neale et al.*, 2008]. When a parcel ascends, its entropy, denoted S, is governed by the following equation:

$$\frac{\partial mS}{\partial z} = \frac{\partial m}{\partial z}\bar{S} = \varepsilon \bar{S} \tag{2}$$

where m is the parcel's mass, with a value of unity at the level of origin (or cloud base), and ε is the mass entrained per unit height into the parcel from its environment. $\bar{S}$ is the entropy of the environmental air. The mass entrainment is assumed constant at 1 per km due to entrainment of the environmental air. Such a linear increase of mass with height implies that the fractional entrainment rate $\frac{1}{m}\frac{\partial m}{\partial z}$ decreases with height as $1/z$ with a cloud base value of 1×10^{-3} m^{-1}. This is qualitatively consistent with some cloud-resolving model estimates of entrainment rates [*Gregory*, 2001].

[7] The air parcel is assumed saturated above the lifting condensation level. Thus, once the entropy of the parcel at each height is obtained from equation (2), it can be inverted to obtain the parcel's temperature and specific humidity. The latent heat from freezing is also included in CAPE calculation. Here a maximum of 1 g kg^{-1} of liquid water is allowed to be retained in the parcel, the rest raining out. Above the freezing level, all liquid water freezes instantly and the latent heat of freezing is used to increase the parcel's temperature. Again, these modifications are the same as those used in the NCAR CAM3.5 [*Neale et al.*, 2008]. The assumption that all liquid water freezes instantly once below 0°C may be unrealistic and may exaggerate the effect of freezing on CAPE. Both observations and cloud modeling studies [*Heymsfield et al.*, 2005; *Phillips et al.*, 2007] suggest that water drops do not freeze homogeneously until about −35°C, above which only a portion of the liquid

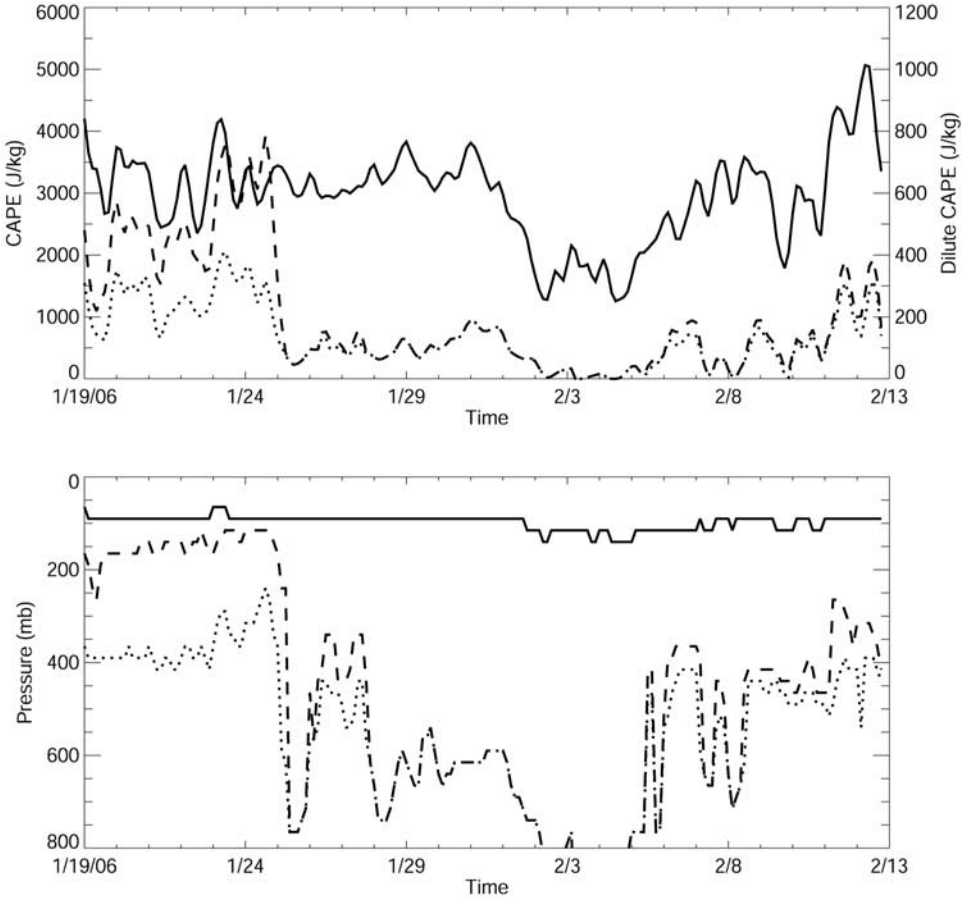

Figure 1. (top) Time series of CAPE and (bottom) neutral buoyancy level for the TWP-ICE IOP. Solid line is for undiluted CAPE calculation, dashed line is for dilute CAPE calculation with freezing-heating, and dotted line is for dilute CAPE calculation without freezing. Dilute CAPE is scaled on the right.

water freezes through heterogeneous freezing. We will perform some limited sensitivity test of this effect later.

[8] Three closure assumptions are examined:

$$\left(\frac{\partial CAPE}{\partial t}\right)_{cu} = -\frac{CAPE - CAPE_0}{\tau}, \tag{3}$$

$$\frac{\partial CAPE}{\partial t} = \left(\frac{\partial CAPE}{\partial t}\right)_{cu} + \left(\frac{\partial CAPE}{\partial t}\right)_{ls} \approx 0, \tag{4}$$

$$\frac{\partial CAPE_e}{\partial t} = \left(\frac{\partial CAPE_e}{\partial t}\right)_{cu} + \left(\frac{\partial CAPE_e}{\partial t}\right)_{ls} \approx 0, \tag{5}$$

where $CAPE_0$ is the threshold value of CAPE above which convection is allowed, τ is the relaxation time, subscripts *ls* and *cu* denote CAPE changes due to large-scale and convective-scale processes respectively, and subscript e denotes environmental contribution to CAPE changes. Here "large-scale processes" is defined loosely as the sum of advection, nonconvective cloud condensation, radiation, and PBL transport, etc., that is, everything other than convection. The first equation (equation (3)) is a CAPE-based closure, the second one is the conventional quasi-equilibrium closure and the third one is the free tropospheric quasi-equilibrium closure. Both the actual CAPE change and the large-scale contribution to the CAPE change can be computed using the observational data. The CAPE changes due to convection are obtained as the difference.

3. Results

3.1. Effect of Entrainment on CAPE

[9] Entrainment of environmental air affects CAPE in two ways. It reduces the buoyancy of the air parcel by bringing in low moist static energy (i.e., dry air) into the parcel. It also reduces the height where the parcel reaches the neutral buoyancy. Figure 1 shows the time series of CAPE with and without entrainment dilution and the corresponding level of neutral buoyancy for the TWP-ICE IOP. For dilute CAPE, the CAPE values without freezing and their corresponding neutral buoyancy levels are also plotted. The undiluted CAPE varies in a range from 1000 to 5000 J/kg, while the dilute CAPE is much smaller, varying between 0 and 800 J/kg. The neutral buoyancy level for undiluted CAPE is near 100 mb at all times during the IOP, whereas for dilute CAPE it varies from less than 150 mb to greater than 800 mb. Note that for the first 6 days, the entrainment dilution effect on CAPE and the neutral buoyancy level is not as large as for other times. Examination of the moisture field in the troposphere (not shown) indicates that for the first 6 days, the active monsoon period, the

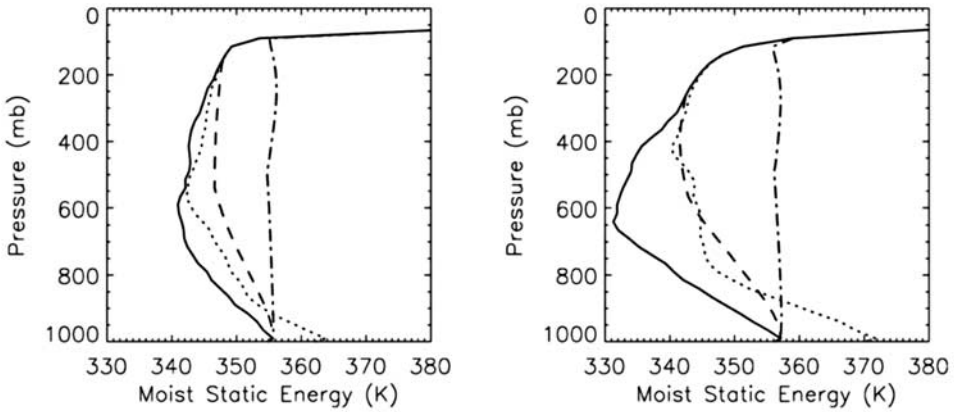

Figure 2. Vertical profiles of observed moist static energy (solid, normalized by c_p) and its saturation value (dotted) for (left) 24 January and (right) 12 February 2006. Moist static energy of parcels lifted from the most unstable level with entrainment (dashed) and without entrainment (dash-dotted) is also shown.

troposphere is relatively moister than other periods. The effect of latent heat of freezing on CAPE and neutral buoyancy level varies widely, depending on how high the neutral buoyancy level is above the freezing level. It can account for as much as 50% of the dilute CAPE, as in the case of the first 6 days, or has no effect at all, as in the case of the middle one-third of the IOP, when the neutral buoyancy level is below the freezing level. The neutral buoyancy level is lowered from 200 mb to 400 mb in the first several days of the IOP when freezing is not considered.

[10] To show the effect of tropospheric moisture on CAPE, Figure 2 displays the moist static energy profiles and their saturation values for day 5 (24 January 2006) and day 24 (12 February 2006), respectively. Also shown are the parcel's moist static energy profiles with and without entrainment dilution. The slight increase of the undiluted parcel's moist static energy above 500 mb is due to latent heating from freezing. 12 February is much drier than 24 January throughout the troposphere, as can be seen from the difference between observed and saturation moist static energy. The undiluted CAPE on 12 February is around 5000 J/kg compared to 3200 J/kg on 24 January. However, when entrainment dilution is included, the parcel's buoyancy, as measured by the difference between the parcel's moist static energy and its environment's saturation moist static energy, is positive from 900 mb to 200 mb, whereas for 12 February the parcel's buoyancy is positive from 850 mb to 650 mb and then becomes small aloft, alternating in sign. This results in dilute CAPE on 24 January more than twice as large as that on 12 February (Figure 1).

[11] To demonstrate the combined effect of entrainment and tropospheric moisture on CAPE, we use the observed temperature and moisture profiles on 12 February and vary the moisture profile according to

$$q_{mod} = q + f(q_s - q), \tag{6}$$

where q is the observed specific humidity and q_s is the saturation specific humidity at observed temperature, f is the factor controlling the degree of subsaturation of the modified moisture profile. $f = 0$ corresponds to the observed moisture profile and $f = 1$ corresponds to the saturation moisture profile. When $f < 0$, the modified moisture profile is drier than observed. The modified specific humidity q_{mod} together with the observed temperature are used to compute CAPE for different values of f and entrainment rates. Figure 3 shows CAPE as functions of f and entrainment rates. When there is no entrainment, CAPE increases from 5000 to over 10000 J/kg when the tropospheric air goes from the observed humidity to saturation. When entrainment is considered, CAPE drops precipitously for entrainment rates up to 0.2×10^{-3} m^{-1}. Further increase in entrainment rate results in a more gradual decrease in CAPE. At entrainment rate of 1×10^{-3} m^{-1}, CAPE is more sensitive to the degree of subsaturation than to entrainment rate. It varies by almost a factor of 10, from the observed 270 J/kg to 2500 J/kg when the air is saturated.

[12] In Figure 3, the moisture variation factor is applied throughout the troposphere. Thus, for a given entrainment

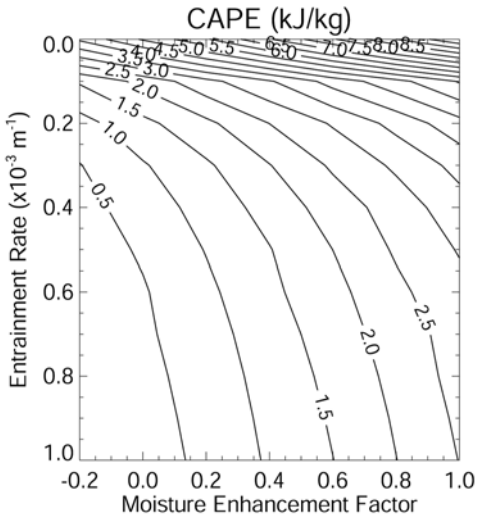

Figure 3. CAPE as function of entrainment rate and moisture enhancement factor f. $f = 0$ corresponds to observed moisture profile and $f = 1$ corresponds to saturation moisture profile at observed temperature for the 12 February 2006 sounding.

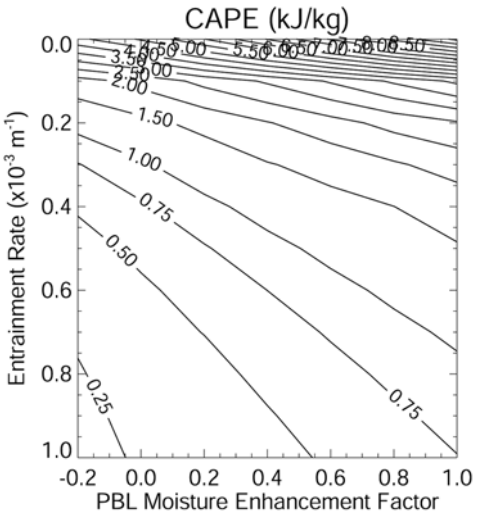

Figure 4. Same as in Figure 3 except that the moisture modification is applied to the boundary layer only.

rate, the increase of CAPE with increasing moisture is a combined effect of both increased moist static energy of the air parcel at its lifting level and a less efficient dilution due to moister air being entrained from the parcel's environment. Figure 4 shows the same plot as Figure 3, except that only the boundary layer air (i.e., the air at the parcel's lifting level) is varied according to equation (6). Therefore it depicts the effect of enhancement of PBL moisture on CAPE as functions of entrainment rate. Because of entrainment of dry air, at a given entrainment rate, CAPE increase with PBL moisture is not as effective as in Figure 3, where moister air is entrained. Comparison of Figures 3 and 4 indicates that when the environmental humidity is fixed to the observed values, the effect of entrainment rate is more dramatic than in Figure 3 as the PBL moisture increases. For example, at $f = 1$, which means the entire troposphere is saturated in Figure 3 and only the PBL air is saturated in Figure 4, CAPE decreases from 3000 J/kg at entrainment rate of 0.5×10^{-3} m^{-1} to 2500 J/kg at entrainment rate of 1×10^{-3} m^{-1} in Figure 3, whereas in Figure 4 for the same entrainment rate range CAPE decreases by 50% from 1500 J/kg to 750 J/kg.

3.2. Effect of Entrainment on Closure Assumptions

[13] With the above results demonstrating the significance of entrainment dilution and humidity in the troposphere in CAPE calculation, we now turn to examining its impact on convection closure assumptions. Previous studies [*Zhang*, 2002, 2003; *Donner and Phillips*, 2003] have shown that among the three closure assumptions equations (3)–(5), the free tropospheric quasi-equilibrium closure has the best agreement with observations whereas the CAPE-based closure has the least agreement. For example, *Donner and Phillips* [2003] showed that the observed $\partial CAPE_e/\partial t$ in equation (5) deviates the least from zero than $\partial CAPE/\partial t$ in equation (4) or $(\partial CAPE/\partial t)_{cu} + (CAPE - CAPE_0)/\tau$ in equation (3) does, as required by their respective closures. Figure 5 shows an example of convective CAPE consumption versus CAPE plot, which illustrates the (lack of) accuracy of the CAPE-based closure using undiluted CAPE for the TWP-ICE IOP. The correlation coefficient and linear regression equation are given in the plot. There is virtually no relationship between CAPE and the convective removal of CAPE. When entrainment dilution is included, the CAPE-based closure is in somewhat better agreement with observations. Figure 6 shows, for dilute CAPE, the scatterplots of CAPE consumption by convection versus CAPE for the SGP97 IOP, COARE IOP and TWP-ICE IOP, respectively. For all three IOPs the correlation coefficients between CAPE and the CAPE removal rate by convection are around 0.5 to 0.6. The relaxation time (the inverse of the linear regression coefficient) ranges from 3 to 5 hours. Although this is a significant improvement over the relationships for undiluted CAPE, the explained variance (r^2) of approximately 30% by the relationships is far from satisfactory for convection closure.

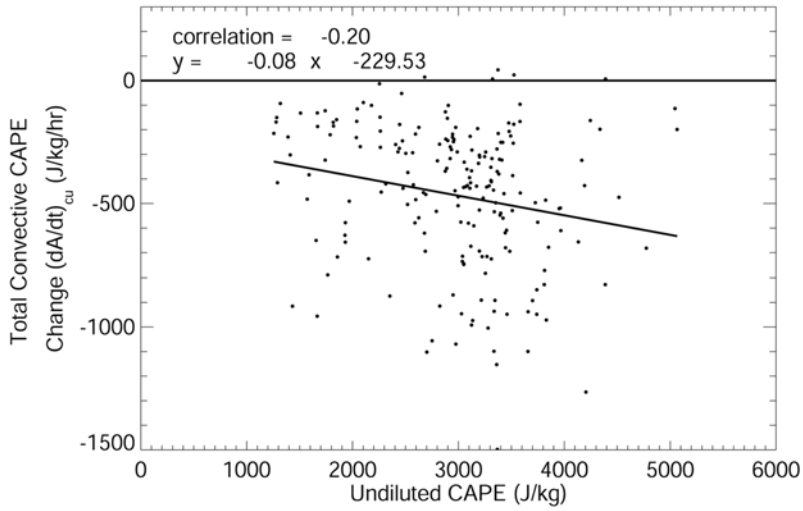

Figure 5. Scatterplot of convective CAPE change versus CAPE using undiluted CAPE calculation for TWP-ICE IOP. Correlation coefficient and linear regression equation are given as well. Each point represents a 3-hour average, and the solid line is the best fit.

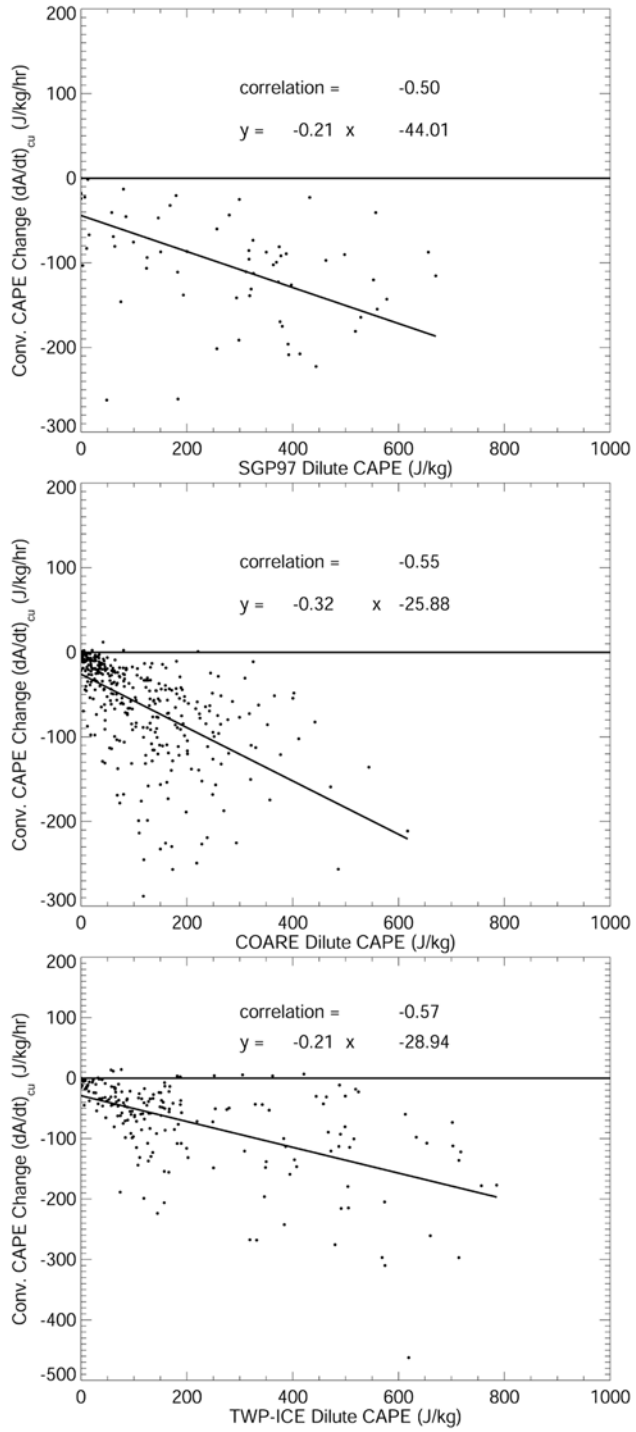

Figure 6. Scatterplot of convective CAPE change versus CAPE using dilute CAPE calculation for (top) SGP97, (middle) COARE, and (bottom) TWP-ICE IOPs. Correlation coefficients and linear regression equations are given, with the reciprocal of the coefficient in the x-term representing the relaxation time in CAPE-based closure. Each point represents a 3-hour average for SGP97 and TWP-ICE and a 6-hour average for COARE. The solid line represents the best fit.

[14] In contrast, Figure 7 shows the scatterplots of CAPE change due to convection versus CAPE change due to large-scale forcing for both the conventional [*Arakawa and Schubert*, 1974] quasi-equilibrium and free tropospheric quasi-equilibrium for the three IOPs using dilute CAPE calculation. In previous studies using undiluted CAPE, *Zhang* [2002, 2003] shows that the free tropospheric quasi-equilibrium assumption is in much better agreement with observations than the conventional quasi-equilibrium does due to strong influence of the boundary layer properties on CAPE. This is particularly true over land, where sensible and latent heat fluxes of 300 to 400 Wm^{-2} are common in early afternoon hours. As shown in Figure 7, for dilute CAPE, however, the free tropospheric quasi-equilibrium and the conventional quasi-equilibrium are less distinguishable. Both are in very good agreement with the observations, with correlation coefficients exceeding 0.9 for all three IOPs. Nevertheless, a closer examination can find that for the SGP97 IOP, the plot for the conventional quasi-equilibrium assumption still has more scatter than that for the free tropospheric quasi-equilibrium assumption, indicating that even with strong entrainment dilution, the large changes of the boundary layer properties due to large surface heat and moisture fluxes over land at the SGP still has noticeable influence on CAPE and CAPE change estimates. Note that in the closure by *Arakawa and Schubert* [1974], equilibrium assumption is applied to every member of an ensemble of cloud plumes, each having a characteristic mass entrainment rate. In Figure 7 a single value is used for mass entrainment. Also, note that the entrainment rates for the plumes, particularly deep convection plumes, in Arakawa and Schubert's quasi-equilibrium closure are much smaller than that used in this study. Thus the artificial boundary layer effect is expected to become more significant, closer to the undiluted CAPE situation studied in the study by *Zhang* [2002, 2003].

[15] As pointed out in the Introduction, the dilute CAPE calculation as adopted by the CAM3.5 includes latent heating from freezing, and freezing was assumed to occur instantly once the parcel's temperature reaches 0°C. In reality, it is likely that only partial freezing would occur until homogeneous ice nucleation is possible, at temperatures near −35°C [*Heymsfield et al.*, 2005]. To examine the potential effect of this instant freezing treatment for ice on the quasi-equilibrium assumptions, we recalculate CAPE and CAPE changes by multiplying the following factor

$$g = \min\left(1., \max\left(0., \frac{T_p - T_{freeze}}{-35}\right)\right) \tag{7}$$

to the latent heat from freezing, where T_p is the parcel's temperature in Kelvin, and T_{freez} = 273.16 K. Thus, below −35°C, all liquid water in the parcel freezes instantly; from 0°C to −35°C, the fraction of freezing is linearly proportional to the temperature below 0°C. Figure 8 shows the free tropospheric quasi-equilibrium assumption using the modified dilute CAPE changes. Comparing with the right column of Figure 7, there is no significant difference between the two in terms of the accuracy of the assumption, as measured by the scatter around the diagonal lines. In general, the CAPE change values are smaller with partial freezing than with instant total freezing. However, this is not

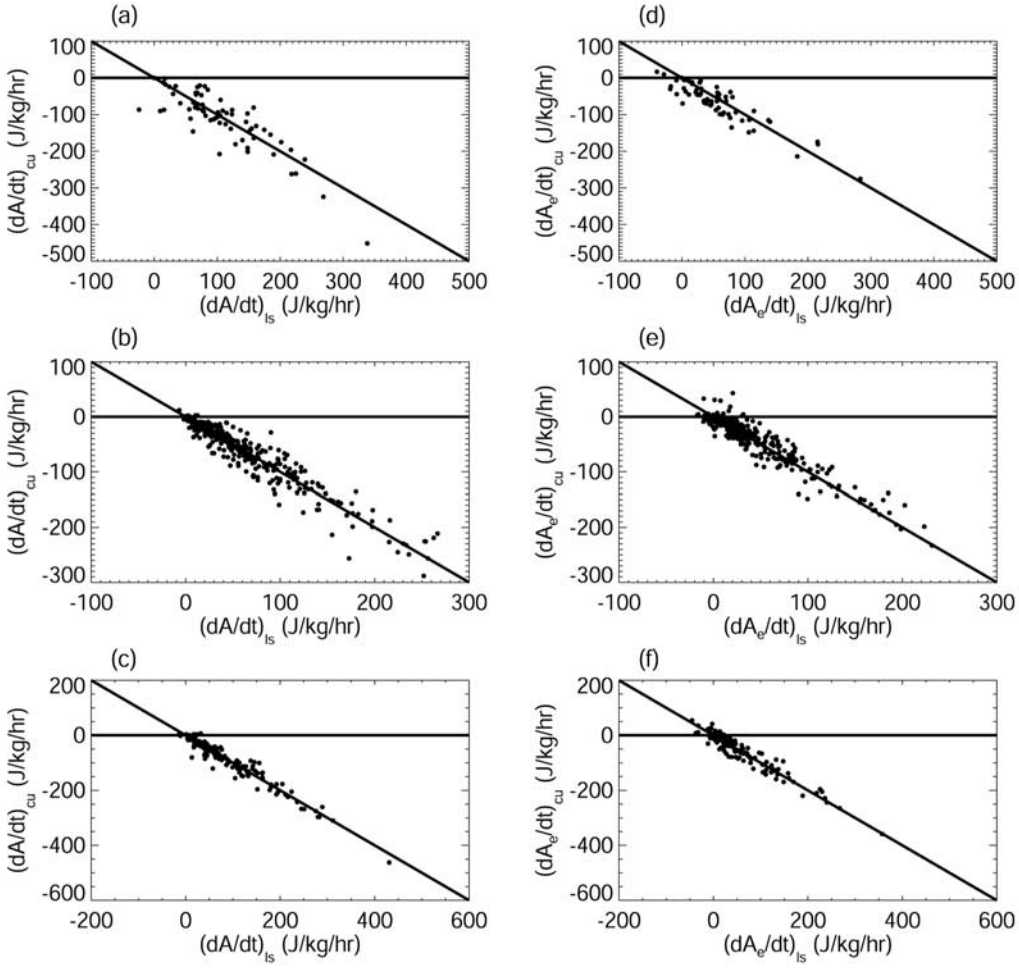

Figure 7. Scatterplots of convective dilute CAPE change versus large-scale dilute CAPE change for (top) SGP97, (middle) COARE, and (bottom) TWP-ICE. In all calculations of CAPE and its change, entrainment dilution of 1 km^{-1} is used. (a–c) Conventional quasi-equilibrium. (d–f) Free tropospheric quasi-equilibrium.

always the case, because the freezing effect on the parcel's buoyancy applies to CAPE calculations both before and after the large-scale forcing is included to obtain the CAPE change. Although CAPE itself is much smaller without freezing, its change due to large-scale forcing may not be small.

[16] Note that the total large-scale forcing on CAPE consists of CAPE change due to free tropospheric large-scale virtual temperature change and that due to parcel's virtual temperature change as a result of boundary layer large-scale processes such as turbulent fluxes [*Zhang*, 2002]:

$$\left(\frac{\partial CAPE}{\partial t}\right)_{ls} = \left(\frac{\partial CAPE_p}{\partial t}\right)_{ls} + \left(\frac{\partial CAPE_e}{\partial t}\right)_{ls}, \qquad (8)$$

where subscript e and p denote environmental contribution and the parcel's contribution, respectively. When entrainment dilution is included, the first term on the rhs of equation (8) is also affected by the environmental temperature and moisture. The similarity between the conventional quasi-equilibrium and the free tropospheric quasi-equilibrium in Figure 7 suggests that for dilute CAPE the total large-scale CAPE forcing and the free tropospheric large-scale CAPE forcing are closely related. Figure 9 presents the scatterplots of these two for the three IOPs, with correlation coefficients and linear regression given in each plot. Indeed, they are highly correlated. For the SGP97 IOP, the free tropospheric large-scale CAPE change accounts for 46% of the total large-scale CAPE change, at a correlation coefficient of 0.72. For both COARE and TWP-ICE, the free tropospheric large-scale CAPE change contribute about 80% to the total large-scale CAPE change, with correlation coefficients over 0.9. Note that for nonconvective periods (defined as precipitation rates <2 mm/day and displayed by crosses in Figure 9), the total large-scale CAPE forcing is most significant in the land case (SGP97), less so in the mixed land-ocean case (TWP-ICE), and least significant in the ocean case (COARE). The free tropospheric large-scale CAPE forcing in all IOP cases for nonconvective periods is small. Their differences, which measure the boundary layer forcing on CAPE, show that even with strong entrainment, the fictitious boundary layer forcing, while already much suppressed compared to

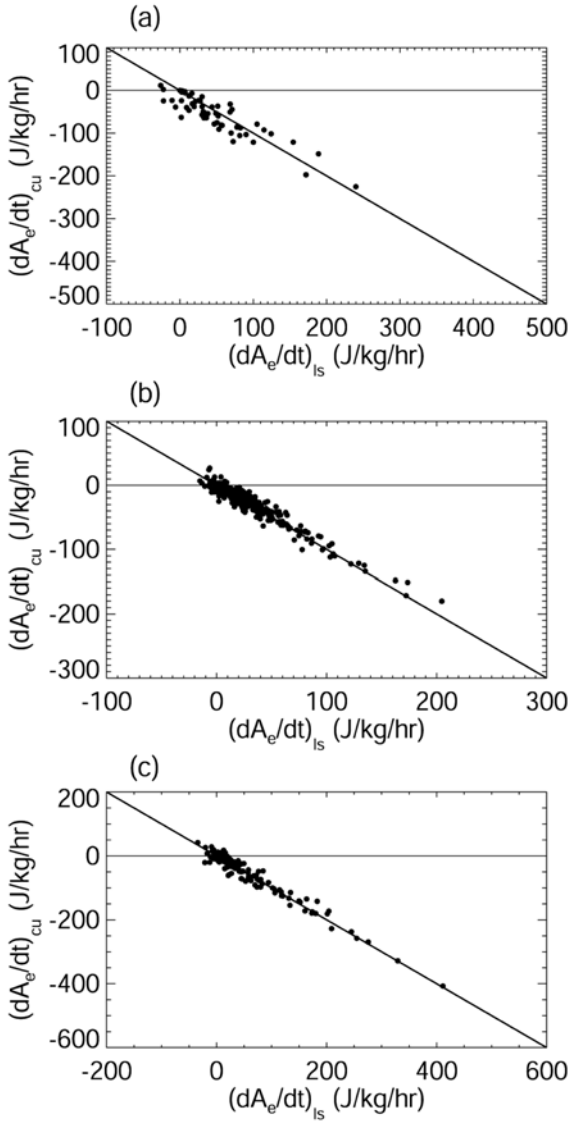

Figure 8. Same as in Figures 7d to 7f, except that the latent heat of freezing is multiplied by the factor given in equation (7).

undiluted CAPE calculation, may still have some non-negligible contamination on convection parameterization.

[17] The impact of entrainment dilution on CAPE change and the quasi-equilibrium assumptions can be understood from the following estimates. The change of boundary layer moist static energy due to surface sensible and latent heat fluxes can be approximated by:

$$c_p \rho \Delta z \frac{\partial h}{\partial t} = F, \tag{9}$$

where c_p is the heat capacity of air, ρ the air density, Δz the boundary layer thickness, and F the sum of surface sensible and latent heat fluxes. For typical boundary layer thickness of 800 m and air density of 1.1 kg/m^3, we have $\frac{\partial h}{\partial t} \approx F/250$ K hour^{-1}. The mean value of the sum of sensible and latent heat fluxes in the TWP-ICE IOP, as estimated from the domain-mean single-column model forcing data set, is 165 W/m^2, which yields a mean moist static energy change rate of 0.66 K/hour in the PBL. We use Figures 2 and 4 for a rough estimate of the resulting CAPE change with and without entrainment dilution. The moist static energy difference between the saturation value and the

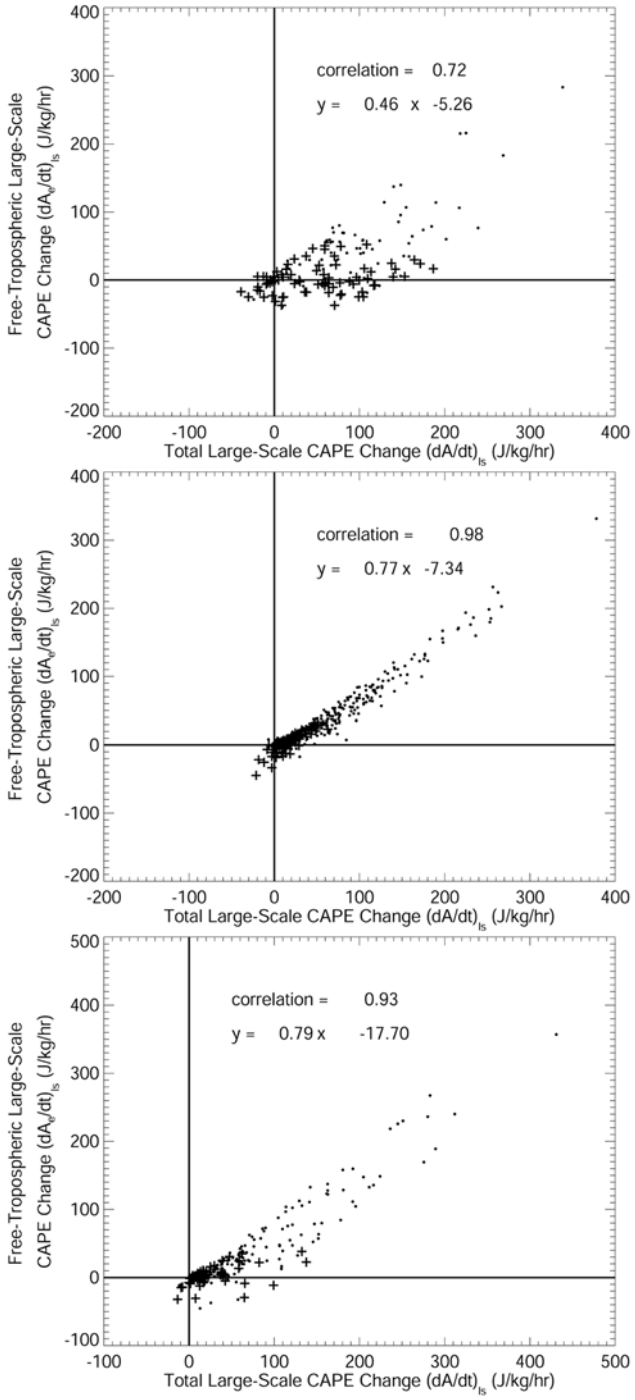

Figure 9. Scatterplots of free tropospheric large-scale dilute CAPE change versus total large-scale dilute CAPE change for (top) SGP97, (middle) COARE, and (bottom) TWP-ICE. Dots are for convective points, and crosses are for nonconvective points. Linear correlation coefficients and regression equations are given in the plots as well.

observed value near the surface is 15 K (372 K − 357 K) according to the right plot in Figure 2. From Figure 4, the CAPE value changes from 270 J/kg when $f = 0$, corresponding to the observed moist static energy profile, to 750 J/kg when $f = 1$, corresponding to saturated moist static energy in the PBL, for dilute CAPE with an entrainment rate of 1×10^{-3} m^{-1}. This yields a 32 J/kg CAPE increase per 1 K increase in PBL moist static energy, or a 21 J/kg/hour CAPE change rate for a 0.66 K/hour PBL moist static energy change due to surface fluxes. For undiluted CAPE calculation, CAPE changes from 5000 J/kg for $f = 0$ to slightly over 10000 J/kg for $f = 1$. This gives a CAPE change rate of 220 J/kg/hour. In other words, with or without the entrainment dilution, the contribution from surface turbulent fluxes to the total CAPE forcing can differ by a factor of 10. On the other hand, the CAPE change due to free tropospheric large-scale forcing is not as sensitive to parcel's entrainment dilution (about a factor of 2 due to its effect on the parcel's neutral buoyancy level), and is typically 200 to 400 J/kg/h (e.g., compare Figure 7 with Figures 6 and 7 in the study by *Zhang* [2003]). Thus consideration of entrainment dilution has a significant impact on the accuracy of convection parameterization closure assumptions as seen in Figure 7. It diminishes the contribution from the boundary layer property changes to CAPE variation. For a 50 mb or 400 m PBL thickness, the above estimated CAPE changes due to surface fluxes would be doubled.

4. Theoretical Interpretation

[18] Section 3 describes the effect of entrainment on CAPE and related convection closure assumptions. This section tries to provide some theoretical interpretation on the observed relationships between convection and large-scale CAPE changes. For undiluted adiabatic ascent of an air parcel lifted from the boundary layer, the large-scale CAPE change can be written as [*Emanuel*, 1994]:

$$\left(\frac{\partial CAPE}{\partial t}\right)_{ls} = \int_{p_t}^{p_b} R_d \left(\frac{\partial T_{vp}}{\partial t} - \frac{\partial T_v}{\partial t}\right)_{ls} d\ln p = (T_b - T_t)\frac{\partial S_b}{\partial t} - \int_{z_b}^{z_t} \left(\frac{g}{c_p}\frac{Q_R}{T} - \frac{g}{\theta}\left(\mathbf{v}\cdot\nabla\theta + \omega\frac{\partial\theta}{\partial p}\right)\right) dz \tag{10}$$

where S is the entropy of air, and is given by $S = c_p \ln T - R_d \ln p + \frac{Lq}{T} - qR_v \ln(RH)$; RH is relative humidity; T is temperature; subscripts b and t stand for the parcel's initial level and the neutral buoyancy level, respectively. Q_R is the radiative heating rate. For simplicity of notations, all quantities represent averages over a large-scale area or a GCM grid box. With the use of hydrostatic relationship and the relationship between potential temperature θ and dry static energy $s = c_p T + gz$, equation (10) can be rewritten as:

$$\left(\frac{\partial CAPE}{\partial t}\right)_{ls} = (T_b - T_t)\frac{\partial S_b}{\partial t} + \frac{R_d}{c_p}\int_{p_t}^{p_b} \left(\left(\mathbf{v}\cdot\nabla s + \omega\frac{\partial s}{\partial p}\right) - Q_R\right) d\ln p. \tag{11}$$

On the right-hand side of equation (11), the first term is due to the parcel's temperature change resulting from surface entropy flux (or sensible and latent heat fluxes), and the second term is due to the environmental or free tropospheric temperature changes resulting from the large-scale forcing. Comparing with equation (8), we have:

$$\left(\frac{\partial CAPE_p}{\partial t}\right)_{ls} = (T_b - T_t)\frac{\partial S_b}{\partial t}, \tag{12}$$

$$\left(\frac{\partial CAPE_e}{\partial t}\right)_{ls} = \frac{R_d}{c_p}\int_{p_t}^{p_b} \left(\left(\mathbf{v}\cdot\nabla s + \omega\frac{\partial s}{\partial p}\right) - Q_R\right) d\ln p. \tag{13}$$

[19] On the other hand, the large-scale dry static energy equation can be written as [*Yanai et al.*, 1973]:

$$Q_1 \equiv \frac{\partial s}{\partial t} + \mathbf{v}\cdot\nabla s + \omega\frac{\partial s}{\partial p} = Q_R - \frac{\partial \overline{s'\omega'}}{\partial p} + L(c - e), \tag{14}$$

where the perturbation product term represents eddy, including convective, transport averaged over a large-scale area. $Q_1 - Q_R \equiv -\partial\overline{s'\omega'}/\partial p + L(c - e)$ is often interpreted as the collective effect of convection except in the boundary layer where turbulent heat flux becomes important. Equation (14) has been used in many studies to diagnose convective heating [e.g., *Yanai et al.*, 1973; *Thompson et al.*, 1979; *Lin and Johnson*, 1996]. Integrating from the surface to the top of convection layer gives

$$P = \int_{p_T}^{p_0} \frac{1}{g}(c - e)dp = \frac{1}{Lg}\int_{p_T}^{p_0} \left(\left(\frac{\partial s}{\partial t} + \mathbf{v}\cdot\nabla s + \omega\frac{\partial s}{\partial p}\right) - Q_R\right) dp - \frac{F_{sh}}{L}, \tag{15}$$

where P is precipitation, a proxy for convection in convectively active periods, F_{sh} is the surface sensible heat flux, which is small compared to latent heat of precipitation during convection, p_0 and p_T are pressure at the surface and the top of the convection layer, respectively. Note that we distinguish p_T from p_t for later discussions. The difference between surface pressure p_0 and the parcel's lifting level pressure p_b is small, typically about 50 mb or so. Using observations from GARP Atlantic Tropical Experiment (GATE), *Thompson et al.* [1979] show that, in convectively active periods, the leading balance in equation (15) is between precipitation and heat convergence $\int_{p_T}^{p_0} \left(\mathbf{v}\cdot\nabla s + \omega\frac{\partial s}{\partial p}\right) dp$. Comparing equations (13) and (15), one sees that aside from the $\partial s/\partial t$ term and the F_{sh} term, the large-scale free tropospheric CAPE change $(\partial CAPE_e/\partial t)_{ls}$ and P share the same integrand, except that one integrates with respect to p and the other with respect to ln p (or equivalently height). Thus, if the vertical distribution of the integrand is invariant with time, the two quantities are linearly related if p_T and p_t are the same, and the surface sensible heat flux is small compared to precipitation, which is often the case. In reality, the vertical distribution of large-scale advective

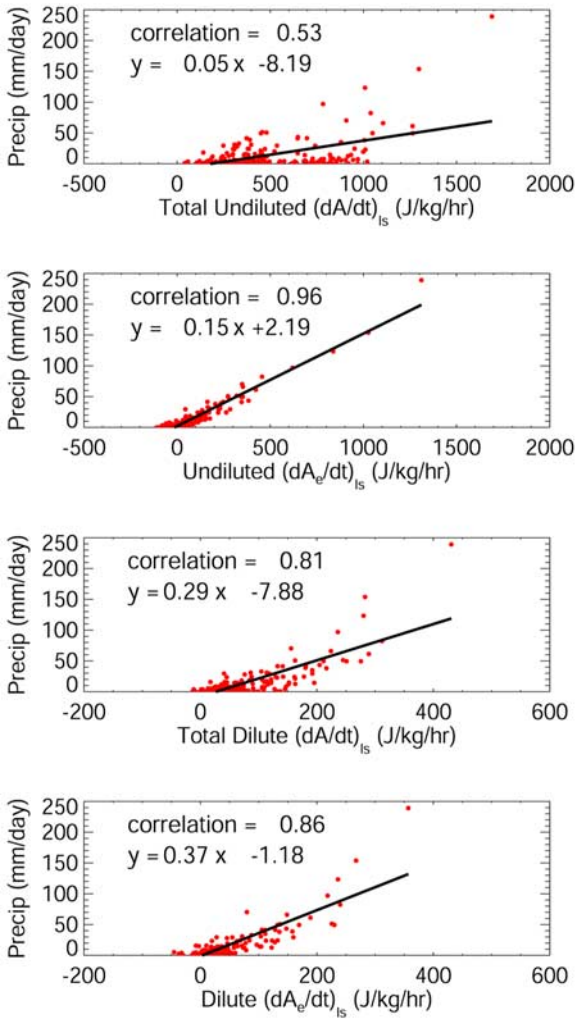

Figure 10. (a, c) Scatterplots of precipitation as functions of total and (b, d) free tropospheric large-scale CAPE changes for undiluted CAPE and dilute CAPE for the TWP-ICE IOP. Correlation coefficients and linear regression equations are given as well. The solid line represents the best fit.

and radiative forcing varies with time. Top-heavy large-scale forcing gives larger $(\partial CAPE_e/\partial t)_{ls}$ and bottom-heavy large-scale forcing gives larger precipitation than the linear relationship suggests. Therefore some degree of scatter is expected between the free tropospheric large-scale CAPE forcing and precipitation.

[20] Figure 10 shows the scatterplots between large-scale CAPE change and precipitation for TWP-ICE. For undiluted CAPE changes, because of the large contribution from surface fluxes, the correlation is weak. Note that there are many points with large values of $(\partial CAPE/\partial t)_{ls}$ but nearly zero precipitation. These are all due to surface contributions through equation (12). On the other hand, when precipitation is plotted against the free tropospheric large-scale CAPE change $(\partial CAPE_e/\partial t)_{ls}$, the correlation is very high (0.96), as expected from equations (13) and (15). Note that the neutral buoyancy level p_t in undiluted CAPE calculation is near 100 mb (Figure 1). Both the theoretical consideration, equations (13) and (15), and the observational results indicate that convection are related to the free tropospheric large-scale forcing on CAPE.

[21] When entrainment dilution is included, CAPE change due to large-scale forcing cannot be calculated from equation (13) alone because the parcel's temperature now also depends on the environmental temperature and moisture that the entrained air possesses. Instead, it is calculated by taking the difference of CAPE with and without the large-scale forcing, holding the parcel's originating level temperature and moisture constant. On the other hand, whether or not entrainment dilution is considered, precipitation is the same and is diagnostically equal to that given in equation (15). Figures 10c and 10d show that the correlation with precipitation is improved for the total large-scale CAPE change, but degraded for the free tropospheric CAPE change, so that the two become comparable. Furthermore, there is large deviation from the linear regression line for heavy precipitation events. As shown earlier, the surface contribution is reduced dramatically by the entrainment dilution, so that the total CAPE change is dominated by the free tropospheric change. The degradation in linear regression correlation by the entrainment dilution for the free tropospheric contribution can be explained by two factors. First, when entrainment is included, the neutral buoyancy level p_t is lower, which decreases the integration range although the integrand (the large-scale temperature forcing) remains the same. This reduces the contribution from the free tropospheric large-scale forcing. Second, the parcel's temperature also depends on the temperature and moisture of the entrained free tropospheric air. When there is large-scale cooling in the free troposphere, a parcel with the same lifting level properties will be colder than without the large-scale free tropospheric cooling due to entrainment. This further reduces the CAPE change from large-scale forcing, and the reduction is larger for stronger forcing. Consequently, we see the large deviation from the linear regression for large rainfall rates. Despite the nonlinear relationship between dilute CAPE change and precipitation, the quasi-equilibrium between large-scale changes and convective changes of dilute CAPE still works well in all three IOPs as seen in Figure 7. This is because similar nonlinear relationships exist between precipitation and resulting convective removal of dilute CAPE due to heating in the free troposphere.

[22] It should be pointed out that the relationship between convection and large-scale free tropospheric CAPE forcing $(\partial CAPE_e/\partial t)_{ls}$, as demonstrated through equations (13) and (15), is a diagnostic one. It does not address the causality issue, that is, whether one is the cause of the other, or vice versa. As the convection and large-scale circulation are highly interactive, this ambiguity in causality also reflects two different angles of view. From a dynamic point of view, to generate large-scale vertical circulation, one needs to specify diabatic heating such as that associated with convection, as is often the case in simple dynamic models such as the Gill model for tropical circulation [*Gill*, 1980]. From physical process modeling point of view, such as in cloud-resolving models or single-column models [*Randall et al.*, 1996], large-scale vertical velocity (or large-scale forcing) needs to be specified in order to produce convection. Therefore it is not clear at all whether convection and large-scale circulation can be separated into cause and

effect. In reality, both are the causes and the effects at the same time. Fortunately, convection closure, by its nature, is to develop an empirical relationship between the observed or predicted large-scale fields and convection to close the parameterization, and does not require one to address the causality issue explicitly, at least for the situation when convection and large-scale fields are in equilibrium.

5. Summary and Discussions

[23] This study investigates the effects of entrainment dilution on CAPE and closure assumptions in convection parameterization. The sounding data from three IOPs (COARE, SGP97 and TWP-ICE) are used for this purpose following the methodology of *Zhang* [2002]. It is shown that entrainment of the environmental air has a strong dilution effect on CAPE. For an entrainment rate of 1 per km, the dilution can reduce CAPE by a factor of 10 or more. The dilution effect depends strongly on the degree of subsaturation of the entrained air: the drier the entrained air, the larger the effect. The dilute CAPE has a moderate correlation of 0.5 to 0.6 with convective removal of CAPE. While better than for undiluted CAPE, this correlation, which only explains about 30% of the variance, is not satisfactory enough for convection closure. On the other hand, while free tropospheric quasi-equilibrium is a superior closure for convection when undiluted CAPE is used as demonstrated in previous studies, both the Arakawa-Schubert quasi-equilibrium closure and the free tropospheric quasi-equilibrium closure work equally well for dilute CAPE in all three IOPs studied. It is further shown from the definition of undiluted CAPE and the large-scale temperature budget equation that free tropospheric large-scale CAPE change and precipitation are linearly related. The results and theoretical arguments presented in the paper show that the most important effect of considering entrainment dilution in CAPE calculation and evaluation of convection parameterization closure assumptions is to enhance the role of free tropospheric humidity relative to the boundary layer properties in CAPE and its variation.

[24] There are advantages and disadvantages to consider entrainment dilution as far as the closure assumptions are concerned. For undiluted CAPE, there is a nearly linear relationship between large-scale free tropospheric CAPE forcing and convection. The free tropospheric quasi-equilibrium closure based on this works well in addressing many persistent biases in the NCAR CAM3 and CCSM3 [*Zhang and Mu*, 2005; *Zhang and Wang*, 2006; *Li and Zhang*, 2008]. However, in situations of triggered convection when the free tropospheric large-scale forcing on CAPE is weak or negligible and convection is forced by surface thermodynamic fluxes, the free tropospheric quasi-equilibrium assumption will not work. For dilute CAPE, under such circumstances surface flux forcing on CAPE will become relatively important, and the conventional quasi-equilibrium assumption incorporates such forcing in determining convection. On the other hand, when large-scale free tropospheric forcing is dominant, for which case the free tropospheric quasi-equilibrium assumption using undiluted CAPE works well, although both the free tropospheric quasi-equilibrium and the Arakawa-Schubert quasi-equilibrium work reasonably well, there are a number of potential factors that can affect the accuracy of the assumption. First, the neutral buoyancy level p_t in dilute CAPE calculation is lower than the top of the large-scale forcing layer in the troposphere p_T. Therefore the forcing in the layer between p_t and p_T is not reflected in the dilute CAPE change. There are a number of occasions during TOGA COARE and SGP97 when dilute CAPE is zero and yet significant precipitation is observed (not shown). In such cases, convection will be underpredicted with dilute CAPE. Second, including the boundary layer contribution, however small it may be, represents a contamination to the actual relationship between precipitation and large-scale CAPE change. Therefore it will also introduce errors in predicted convection.

[25] All the results presented in this study are averages over the observational domain typical of today's GCM grid size (200 to 300 km). Therefore the closures examined are suitable for such GCM resolutions. As the model resolution increases, how does it affect a particular closure? In CAPE-based closure, since CAPE is not very sensitive to model grid size (the mean state variables only vary gradually, particularly over oceans), convection so parameterized has less scale dependence. On the other hand, observed precipitation is highly scale-dependent. On smaller scales, precipitation is more intense. To incorporate such scale dependence into convection parameterization, a typical practice in global modeling is to "tune" the free parameters in the parameterization scheme, such as adjusting the relaxation timescale in CAPE-based closure for different model resolutions. In contrast, in quasi-equilibrium closures the large-scale advective forcing, which largely determines convection, highly depends on the model resolution: the smaller the grid size the larger the advective forcing, and thus the more intense the convection. Therefore the convection parameterization has the scale dependence built into it. As such, the quasi-equilibrium–based parameterization should work well as GCM resolution increases.

[26] **Acknowledgments.** This research was supported by the Biological and Environmental Research Program (BER), US Department of Energy under grant DE-FG02-03ER63532, and by the US National Science Foundation grants ATM-0601781 and ATM-0832915. The author benefited greatly from discussions with Leo Donner, Phil Rasch, Steve Klein, David Neelin, Xiaoqing Wu, Minghua Zhang, and Rich Neale, as well as with many others of the NCAR CAM3 model development team and the Atmospheric Model Working Group of the CCSM3. Zhiqiu Gao helped implement Rich Neale's dilute parcel temperature calculation code obtained from the CAM3.5 at the early stage of this research. The author thanks the anonymous reviewers for their valuable comments.

References

Arakawa, A. (2004), The cumulus parameterization problem: Past, present and future, *J. Clim.*, *17*, 2493–2525.

Arakawa, A., and W. H. Schubert (1974), Interaction of a cumulus cloud ensemble with the large-scale environment. part I, *J. Atmos. Sci.*, *31*, 674–701.

Ciesielski, P. E., L. M. Hartten, and R. H. Johnson (1997), Impacts of merging profiler and rawinsonde winds on TOGA COARE analyses, *J. Atmos. Oceanic Tech.*, *14*, 1264–1279.

Collier, J. C., and G. J. Zhang (2006), Simulation of the North American monsoon by the NCAR CCM3 and its sensitivity to convection parameterization, *J. Clim.*, *19*, 2851–2866.

Donner, L. J., and V. T. Phillips (2003), Boundary layer control on convective available potential energy: Implications for cumulus parameterization, *J. Geophys. Res.*, *108*(D22), 4701, doi:10.1029/2003JD003773.

Emanuel, K. A. (1994), *Atmospheric Convection*, 580 pp., Oxford Univ. Press, New York.

Gill, A. E. (1980), Some simple solutions for heat-induced tropical circulation, *Q. J. R. Meteorol. Soc.*, *106*, 447–462.

Gregory, D. (2001), Estimation of entrainment rate in simple models of convective clouds, *Q. J. R. Meteorol. Soc.*, *127*, 53–72.

Gregory, D., J.-J. Morcrette, C. Jacob, A. C. M. Beljaars, and T. Stockdale (2000), Revision of convection, radiation and cloud schemes in the ECMWF Integrated Forecasting System, *Q. J. R. Meteorol. Soc.*, *126*, 1685–1710.

Heymsfield, A. J., L. M. Miloshevich, C. Schmitt, A. Bansemer, C. Twohy, M. R. Poellot, A. Frindland, and H. Gerber (2005), Homogeneous ice nucleation in subtropical and tropical convection and its influence on cirrus anvil microphysics, *J. Atmos. Sci.*, *62*, 41–65.

Holloway, C. E., and J. D. Neelin (2009), Moisture vertical structure and tropical deep convection, *J. Atmos. Sci.*, in press.

Li, G., and G. J. Zhang (2008), Understanding biases in shortwave cloud radiative forcing in the National Center for Atmospheric Research Community Atmosphere Model (CAM3) during El Nino, *J. Geophys. Res.*, *113*, D02103, doi:10.1029/2007JD008963.

Lin, X., and R. H. Johnson (1996), Heating, moistening, and rainfall over the western Pacific Warm Pool during TOGA COARE, *J. Atmos. Sci.*, *53*, 3367–3383.

Maloney, E. D., and D. L. Hartmann (2001), The sensitivity of intraseasonal variability in the NCAR CCM3 to changes in convective parameterization, *J. Clim.*, *14*, 2015–2034.

May, P. T., J. H. Mather, G. Vaughan, and C. Jacob (2008), Characterizing oceanic convective cloud systems: The Tropical Warm Pool International Cloud Experiment, *Bull. Am. Meteorol. Soc.*, *89*, 153–155, doi:10.1175/BAMS-89-2-153.

McBride, J. L., and W. M. Frank (1999), Relationship between stability and monsoon convection, *J. Atmos. Sci.*, *56*, 24–36.

Michaud, L. M. (1998), Entrainment and detrainment required to explain updraft properties and work dissipation, *Tellus*, *50A*, 283–301.

Neale, R. B., J. H. Richter, and M. Jochum (2008), The impact of convection on ENSO: From a delayed oscillator to a series of events, *J. Clim.*, *21*, 5904–5924.

Neelin, J. D., O. Peters, J. W.-B. Lin, K. Hales, and C. E. Holloway (2008), Rethinking convective quasi-equilibrium: Observational constraints for stochastic convective schemes in climate models, *Philos. Trans. R. Soc. A*, *366*, 2581–2604.

Phillips, V. T. J., L. J. Donner, and S. T. Garner (2007), Nucleation processes in deep convection simulated by a cloud-system-resolving model with double moment bulk microphysics, *J. Atmos. Sci.*, *64*, 738–761.

Randall, D. A., K.-M. Xu, R. J. C. Somerville, and S. Iacobellis (1996), Single-column models and cloud ensemble models as links between observations and climate models, *J. Clim.*, *9*, 1683–1697.

Raymond, D. (1995), Regulation of moist convection over the west Pacific warm pool, *J. Atmos. Sci.*, *52*, 3945–3959.

Thompson, R. M., Jr., S. W. Payne, E. E. Recker, and R. J. Reed (1979), Structure and properties of synoptic-scale wave disturbances in the intertropical convergence zone of the eastern Atlantic, *J. Atmos. Sci*, *36*, 53–72.

Tiedtke, M. (1989), A comprehensive mass flus scheme for cumulus parameterization in large-scale models, *Mon. Weather Rev.*, *117*, 1779–1800.

Xie, S.-C., and M.-H. Zhang (2000), Impact of the convective triggering function on single-column model simulations, *J. Geophys. Res.*, *105*, 14,983–14,996.

Yanai, M., S. Esbensen, and J. H. Chu (1973), Determination of bulk properties of tropical cloud clusters from large-scale heat and moisture budgets, *J. Atmos. Sci.*, *30*, 611–627.

Zhang, G. J. (2002), Convective quasi-equilibrium in midlatitude continental environment and its effect on convective parameterization, *J. Geophys. Res.*, *107*(D14), 4220, doi:10.1029/2001JD001005.

Zhang, G. J. (2003), Convective quasi-equilibrium in the tropical western Pacific: Comparison with midlatitude continental environment, *J. Geophys. Res.*, *108*(D19), 4592, doi:10.1029/2003JD003520.

Zhang, G. J., and N. A. McFarlane (1991), Convective stabilization in midlatitudes, *Mon. Weather Rev.*, *119*, 1915–1928.

Zhang, G. J., and N. A. McFarlane (1995), Sensitivity of climate simulations to the parameterization of cumulus convection in the Canadian Climate Centre general circulation model, *Atmos. Ocean*, *33*, 407–446.

Zhang, G. J., and M. Mu (2005), Simulations of the Madden-Julian oscillation in the NCAR CCM3 using a revised Zhang-McFarlane convection parameterization scheme, *J. Clim.*, *18*, 4046–4064.

Zhang, G. J., and H. Wang (2006), Toward mitigating the double ITCZ problem in NCAR CCSM3, *Geophys. Res. Lett.*, *33*, L06709, doi:10.1029/2005GL025229.

G. J. Zhang, Climate, Atmospheric Science and Physical Oceanography Division, Scripps Institution of Oceanography, University of California, San Diego, 9500 Gilman Drive, La Jolla, CA 92093-0221, USA. (gzhang@ucsd.edu)